Supplementary Information (SI) for Journal of Materials Chemistry C.
This journal is © The Royal Society of Chemistry 2025

Supplementary Information

Boosting Photoelectricity Based on Self-supported Flexible Metal-organic Framework Arrays for Photo-Fenton like Degradation of Organic Pollutants

Shenghao Wang,‡ Yajuan Wang,‡ Linbo Cao, Jiasheng Zhang, Yuqing Liu, Bo Wang and Mingmin Li*

Life and Health Intelligent Research Institute, Key Laboratory of life health detection, Tianjin University of Technology, Tianjin 300384, P. R. China

‡ S. H. and Y. J. contributed equally to this work.

Corresponding author: mingmin@email.tjut.edu.cn

Methods

The morphology of all materials was characterized by scanning electron microscopy (SEM, Quanta FEG 250) and high-resolution transmission electron microscope (HRTEM, Talos F200 X). Atomic force microscope (AFM, Dimension iconXR) was used to detect the height profiles, lateral dimensions and Young's modulus of the nanosheets. Powder X-Ray diffraction (PXRD) pattern of all materials were collected at ambient temperature with a D/teX Ultra 250 x diffractometer operated at 40 kV and 40 mA using Cu Kα (λ = 1.5418 Å) radiation, with a scan speed of 1 sec/step and a step size of 0.02° in 2θ. Ultraviolet-visible spectrophotometer (Lambda 750 UV/Vis/NIR Perkin Elmer) was used to determine the absorption spectrum of the materials and to analyze the structure and optical absorption properties of the materials. Fourier transform infrared (FT-IR, 97% Frontier Mid-IR FTIR/STA6000-TL9000-Clarus SQ8) spectroscopy was applied to evaluate the membrane surface functional groups. The chemical compositions of CF@Cu-TCPP and CF@Cu, Zn-TCPP were analyzed by an

X-ray photoelectron spectroscopy (ESCALAB250Xi). The charged properties of materials and contaminants in aqueous solutions were analyzed by dynamic light scattering (90Plus Zeta). Electrochemical workstation (N9613A) was applied to analyze the electrochemical impedance and photoelectric response of CF@Cu-TCPP, CF@Cu, Zn-TCPP and 3D Cu-TCPP. Microplate reader (SpectraMax ID3) was used to determine the concentration of pollutants in the solution to determine the concentration of organic contaminants in water.

Material Synthesis Procedures

Preparation of CF@CuO. Cu foam was cut into 2 cm × 5 cm pieces and washed continuously by acetone, ethanol and deionized water. Then they were placed in the oven at 60 ℃ overnight to obtain CF@CuO for further use.

Synthesis of CF@Zn_xCu_yO. Cu foam was cut into 2 cm × 5 cm pieces and washed continuously by acetone, ethanol, deionized water and 1 M hydrochloric acid for 30 min. Then they were placed in the oven at 60 ℃ overnight for further use. The as-obtained CF foam was vertically placed into a stainless-steel autoclave lined with teflon. 10 mL of aqueous solution containing zinc nitrate hexahydrate (15 mM), hexamethylenetetramine (15 mM), and ammonia (0.4 mL) was added and heated then at 90 ℃ for 12 h. After cooling to room temperature naturally, the as-prepared CF@Zn_xCu_yO was obtained by thoroughly rinsed with deionized water and ethanol for 3 times, respectively, and then dried in the oven at 80 ℃ overnight.

Synthesis of CF@Cu-TCPP array (CF@Cu-TCPP). Polyvinylpyrrolidone (20 mg) and pyrrole (0.8 mg) were dissolved in 12 mL of mixture solution (DMF: ethanol = 3:1) to obtain solution A. Solution B was prepared by dissolving 2 mg, 4 mg, 6 mg or 8 mg of TCPP into 4 mL of a mixed solution (DMF: ethanol =3:1) through ultrasound treatment for 20 min. Solution B was then added into solution A and thoroughly mixed before introducing CF@CuO into the threaded scintillation bottle. The screw-capped scintillation bottle was heated at 80 ℃ for 24 h in an oven and cooled to room temperature. The obtained material was washed with ethanol and left to dry naturally

to obtain CF@Cu-TCPP. For the preparation of CF@Cu, Zn-TCPP, similar operation was applied except that of CF@Cu_xZn_yO was used instead of CF@CuO.

Synthesis of 3D Cu-TCPP MOFs. 3D Cu-TCPP MOF was synthesized according to literature reported with slight modification [1]. In brief, a mixture of $Cu(NO_3)_2 \cdot 3H_2O$ (21.6 mg, 0.09 mmol), TCPP (23.7 mg, 0.03 mmol), DMF (4.5 mL) and ethanol (1.5 mL) was added into a small screw-cap vial, and heated at 80 °C for 24 h. After cooling to room temperature, the solution was centrifuged at 10000 r/min for 5 min to separate the product. The obtained purplish-red product was washed 3 times with ethanol and then dispersed and stored in ethanol for further use.

ROS Detection with Electron Paramagnetic Resonance (EPR). The EPR test was performed at room temperature. Pyrazine 5,5-dimethyl-1-pyrroline N-oxide (DMPO) was selected as trapping agent for ·OH and $\cdot O_2^-$, whereas 2,2,6,6-tetramethylpiperidine (TEMP) was used as the trapping agent for $^1O_2$. In brief, CF@Cu, Zn-TCPP was ultrasonically dispersed in 20 mL water (MeOH for $\cdot O_2^-$), into which 50 μL of H_2O_2 (30%) was added. The experiments were carried out in the presence or absence of light. After being stirred for 5 min under the above conditions, 45 μL of the reaction solution was taken out to mix with 5 μL of trapping agents. Then the liquid sample was then aspirated into the capillary. The bottom of the capillary was sealed with vaseline, and the surface of the capillary was wiped clean and put into a paramagnetic tube for testing the production of ROS.

Figures

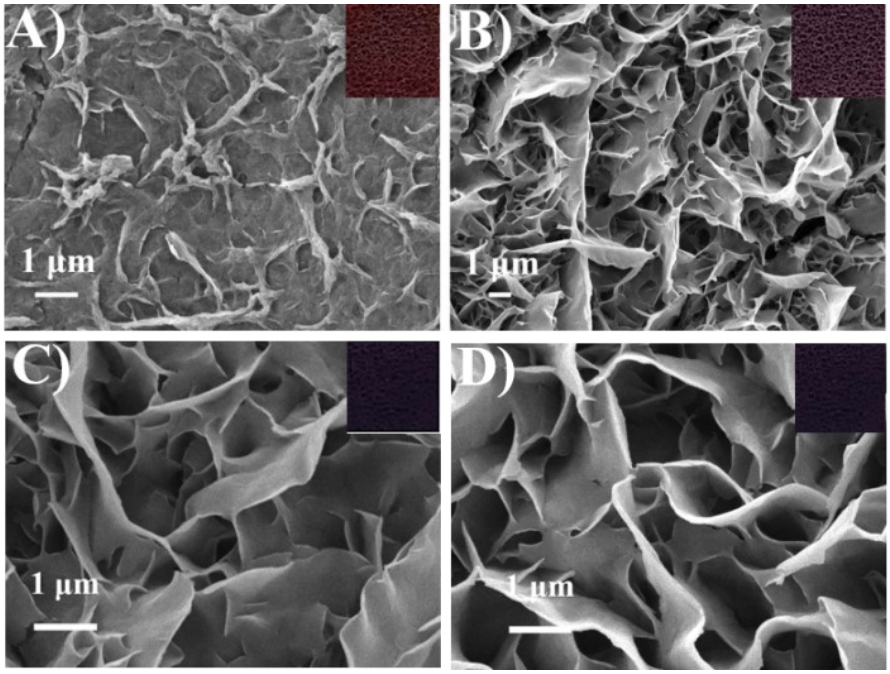

Figure S1. The SEM images of **A)** CF@Cu-TCPP-2, **B)** CF@Cu-TCPP-4, **C)** CF@Cu-TCPP-6 and **D)** CF@Cu-TCPP-8 (**The** TCPP quality is 2 mg, 4 mg, 6 mg and 8 mg, inserts: corresponding material photos).

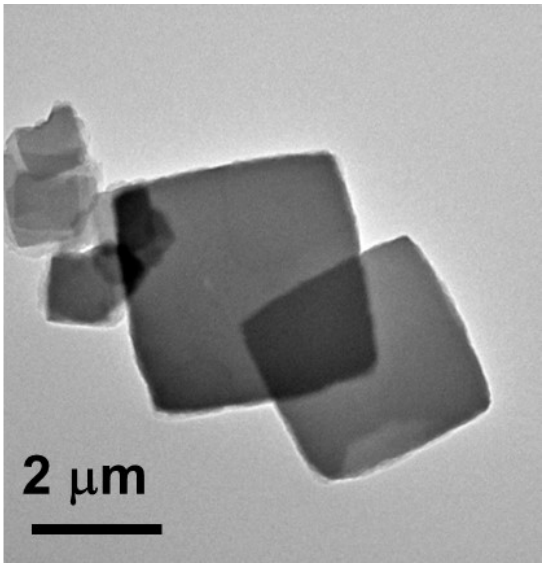

Figure S2. A) TEM image of 3D Cu-TCPP.

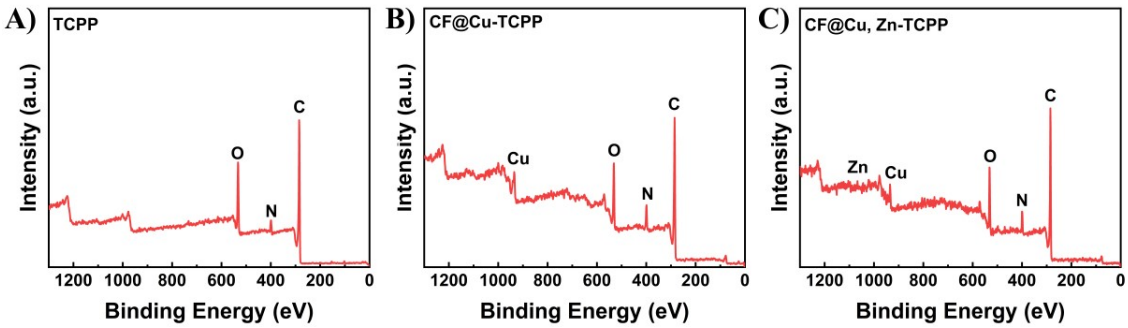

Figure S3. XPS survey spectrums of **A)** TCPP, **B)** CF@Cu-TCPP and **C)** CF@Cu, Zn-TCPP.

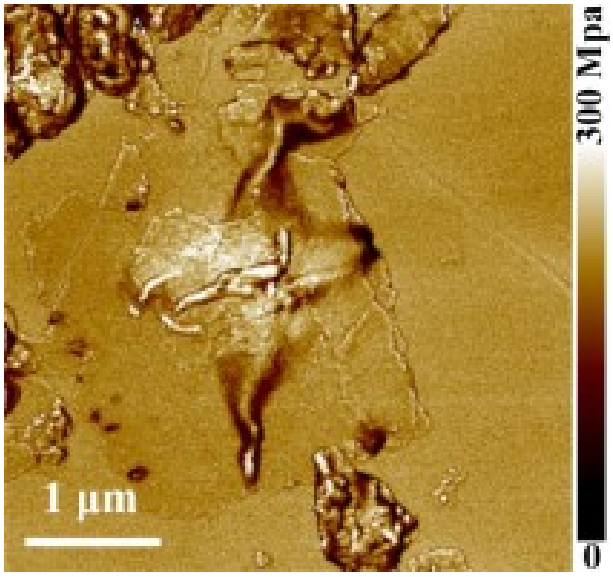

Figure S4. Young's modulus map of Cu, Zn-TCPP characterized by AFM.

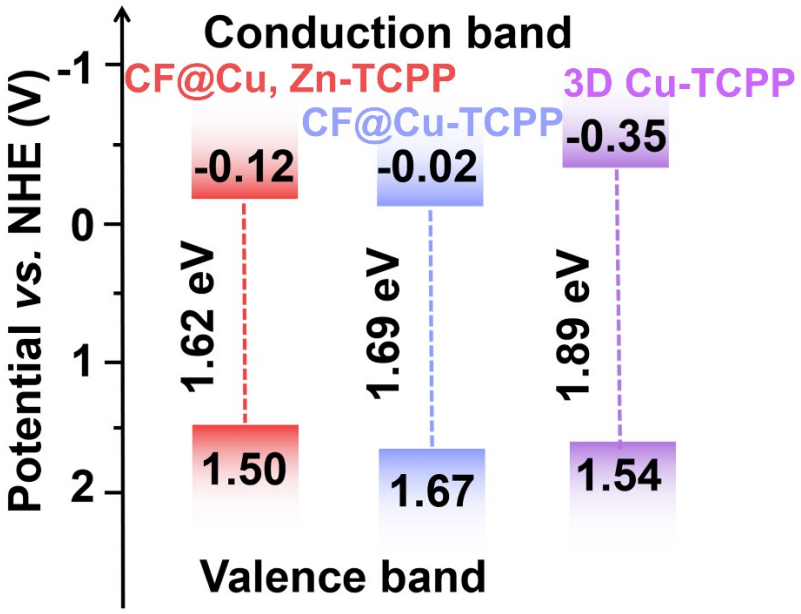

Figure S5. Electronic band structure diagram of 3D Cu-TCPP, CF@Cu-TCPP and CF@Cu, Zn-TCPP.

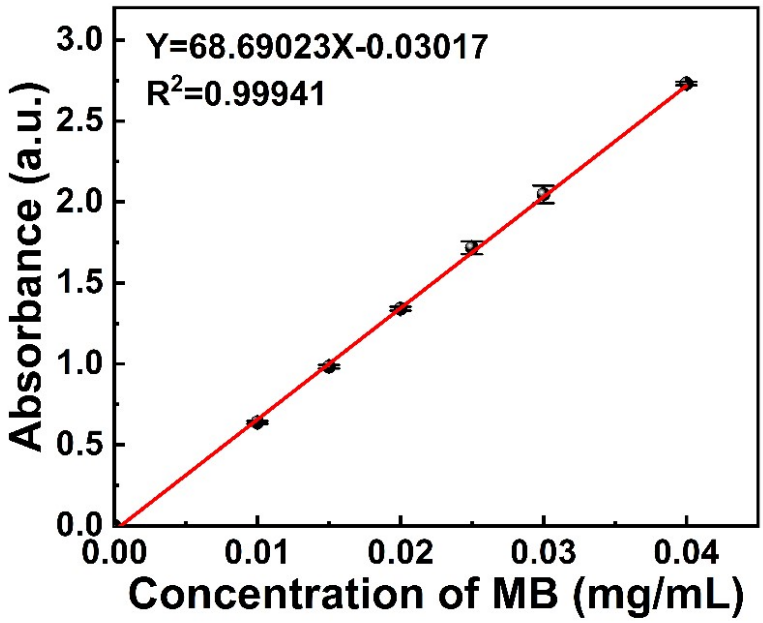

Figure S6. Standard curve of MB determined by UV-vis.

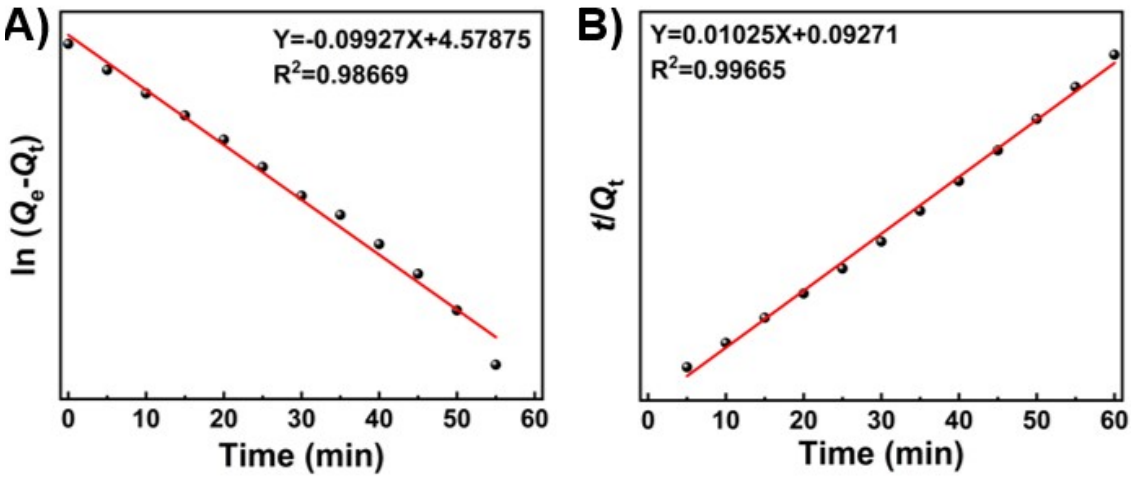

Figure S7. A) Pseudo-first order kinetics model of the MB adsorption process. **B)** Pseudo-second order kinetics model of the MB adsorption process.

Table S1. The adsorption kinetics parameters of MB fitted by different model.

Pseudo-first order kinetics model			
Sample	Q_e (mg·g^{-1})	K_1 (min^{-1})	R^2
MB	97.37915	0.09927	0.98669
Pseudo-second order kinetics model			
Sample	Q_e (mg·g^{-1})	K_2 (min^{-1})	R^2
MB	97.56098	1.13×10^{-3}	0.99665

Table S2. The parameters of Intra-particle diffusion model

Sample	$K_{3,I}$ ($min^{-0.5}$)	$K_{3,II}$ ($min^{-0.5}$)
MB	15.22037	2.35969

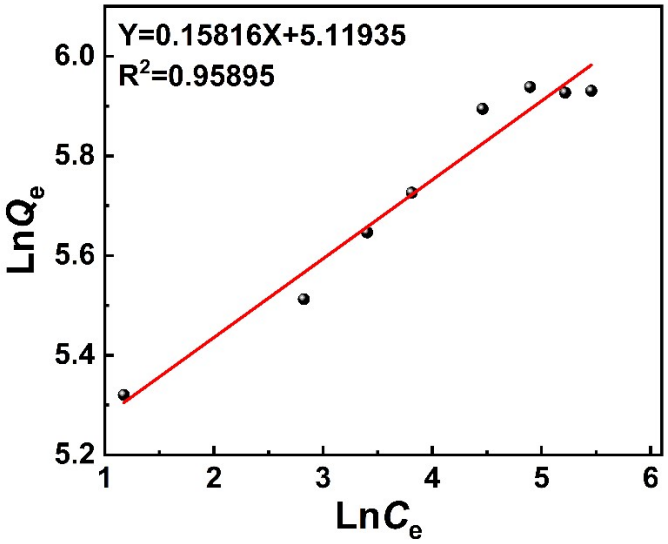

Figure S8. The linear fitting of MB adsorption through Freundlich model.

Table S3. The parameters of adsorption isotherm curve fitted through Langmuir and Freundlich isotherm adsorption model.

Langmuir isotherm model				
Sample	Q_m ($mg \cdot g^{-1}$)	K_L ($L \cdot mg^{-1}$)	R^2	R_L
MB	395.26	0.10446	0.99894	0.02337 (C=400 mg/L)
Freundlich isotherm model				
Sample	K_F	n	R^2	
MB	167.20087	6.32271	0.95895	

Table S4. Statistics of adsorption capacity towards MB by different adsorbents.

Adsorbent	Q_m (mg/g)	References
Fe_3O_4/Mt	106.38	[2]
Fe_3O_4@C	52.63	[3]
Cu-BTC@AG	282.466	[4]
CNC/MnO_2/SA	114.5	[5]
MAAC-800-4	710	[6]
BMHC-H_2O_2	310	[7]
MMT@Ni_4Fe_1LDH	99.18	[8]

PCN-222@PCC-5	125	[9]
Zr-MOF	169	[10]
MOF-235	252	[11]
GNS/Fe_3O_4	43.8	[12]
Al-MIL-101	90	[13]
CF@Cu, Zn-TCPP	395.26	This work

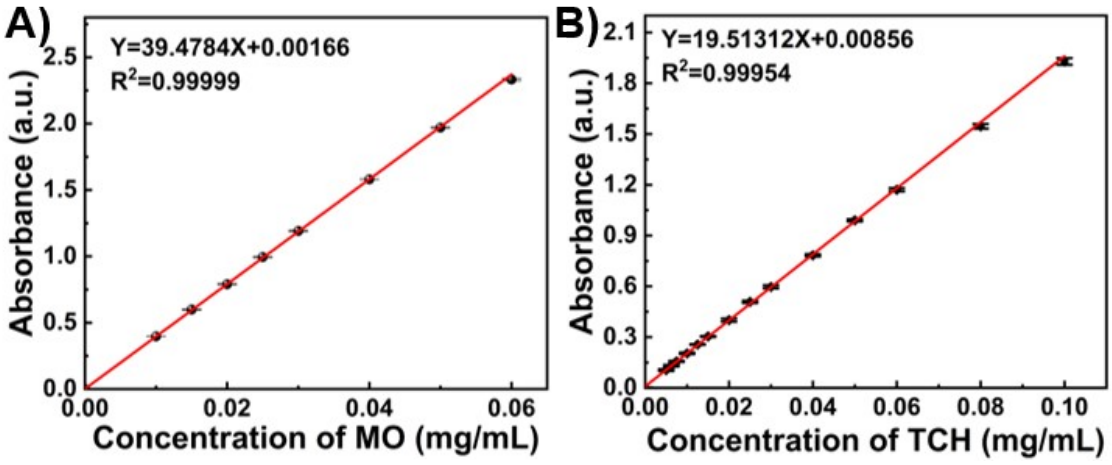

Figure. S9. Standard curve of A) MO and B) TCH determined by UV-vis.

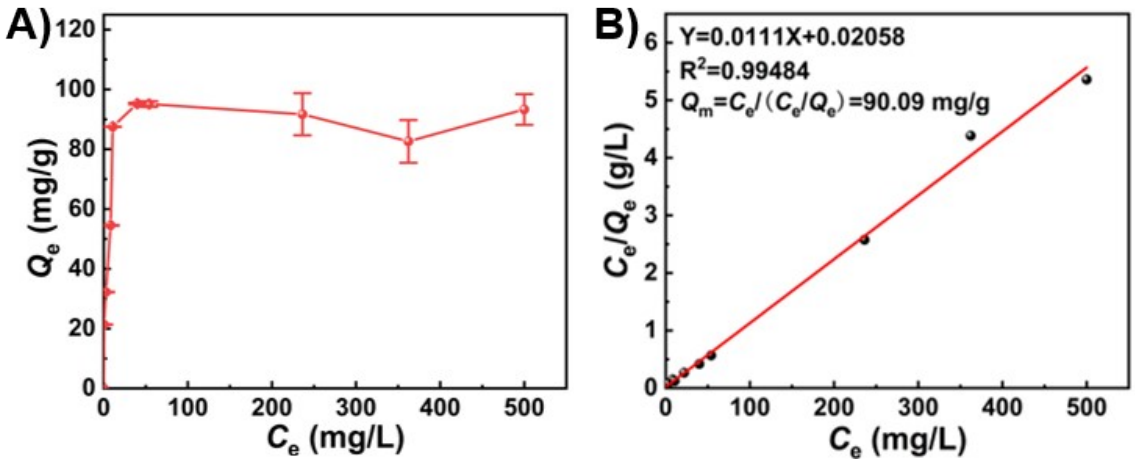

Figure S10. A) The adsorption isotherm of CF@Cu, Zn-TCPP for MO. **B)** The adsorption curve of MO and related parameters fitted by the Langmuir model.

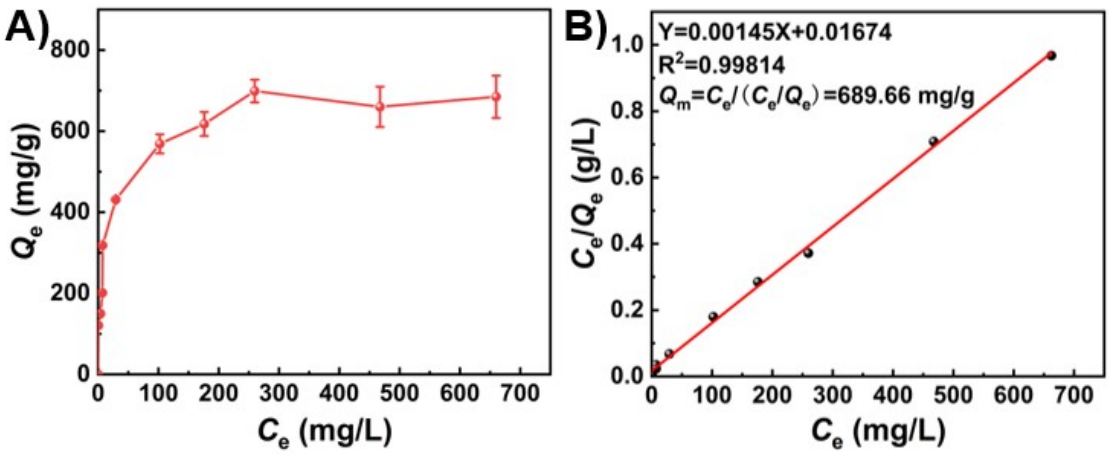

Figure S11. A) The adsorption isotherm of CF@Cu, Zn-TCPP for TCH. **B)** The adsorption curve of TCH and related parameters fitted by the Langmuir model.

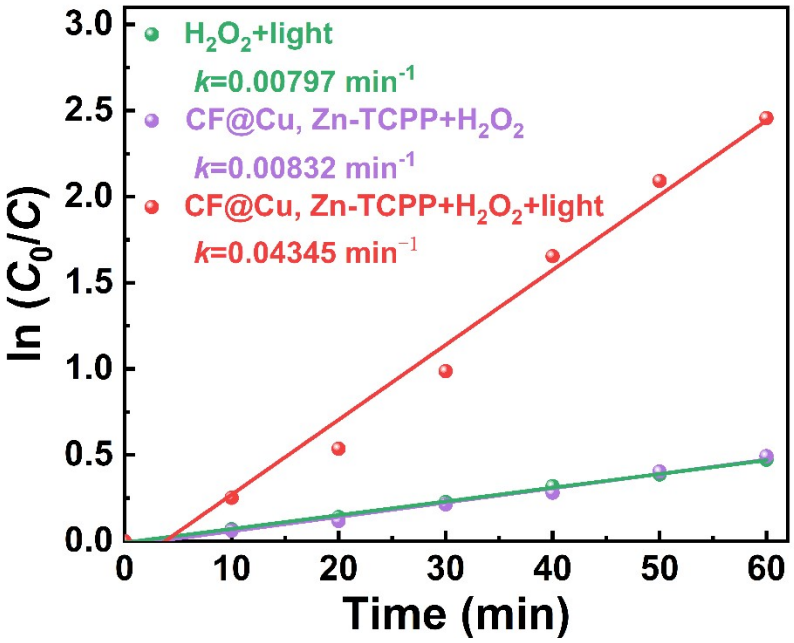

Figure S12. Degradation rate constants of MB under different conditions.

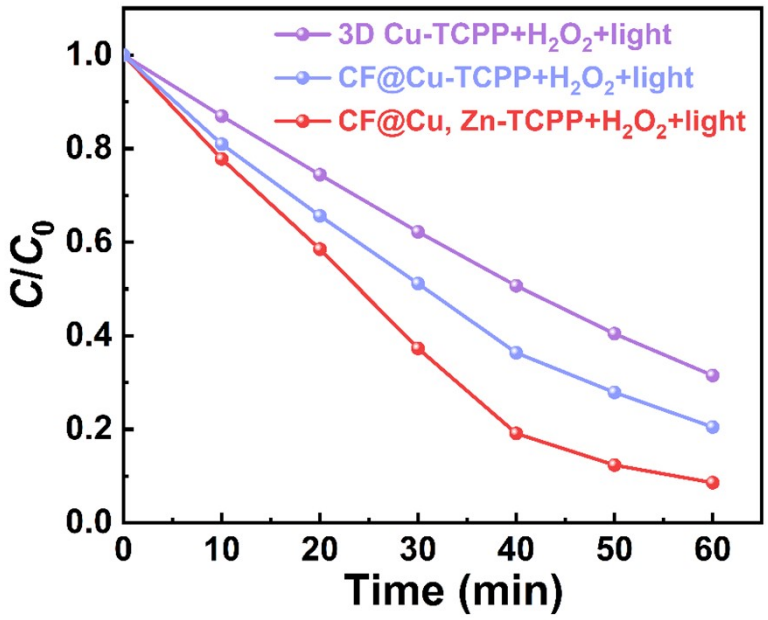

Figure S13. Degradation rate constants of MB by different materials.

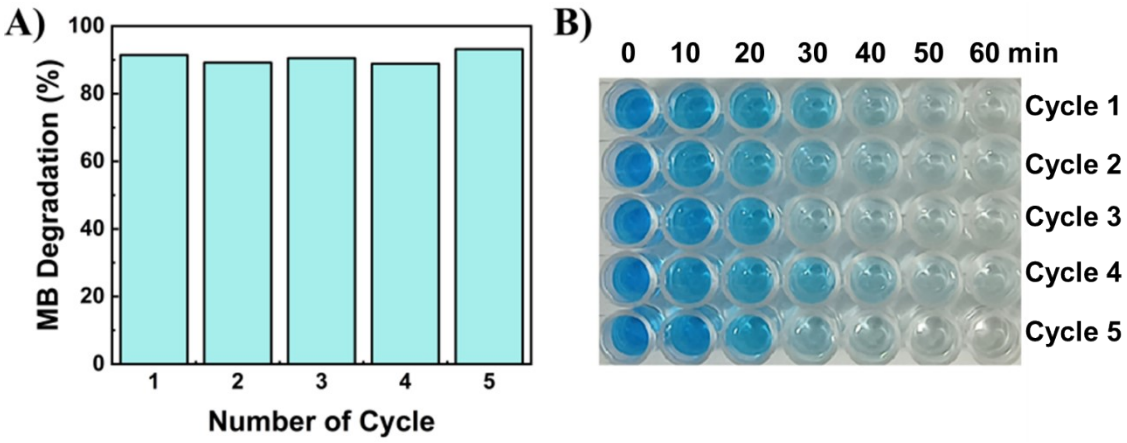

Figure S14. A) Photo-Fenton like degradation efficiency of MB by CF@Cu, Zn-TCPP in five cycles. **B)** The color changes of MB in five degradation cycles.

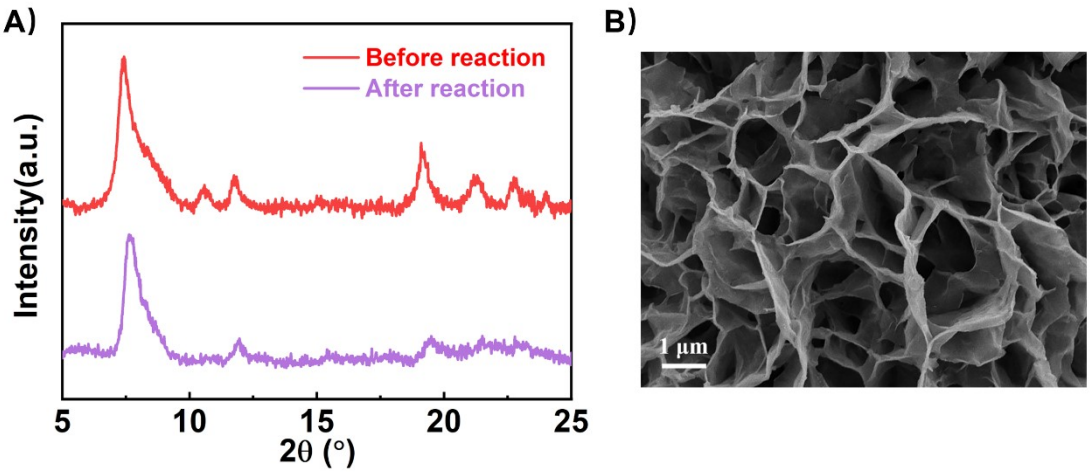

Figure S15. A) PXRD pattern and **B)** SEM image of CF@Cu, Zn-TCPP after photo-Fenton like degradation of MB dyes.

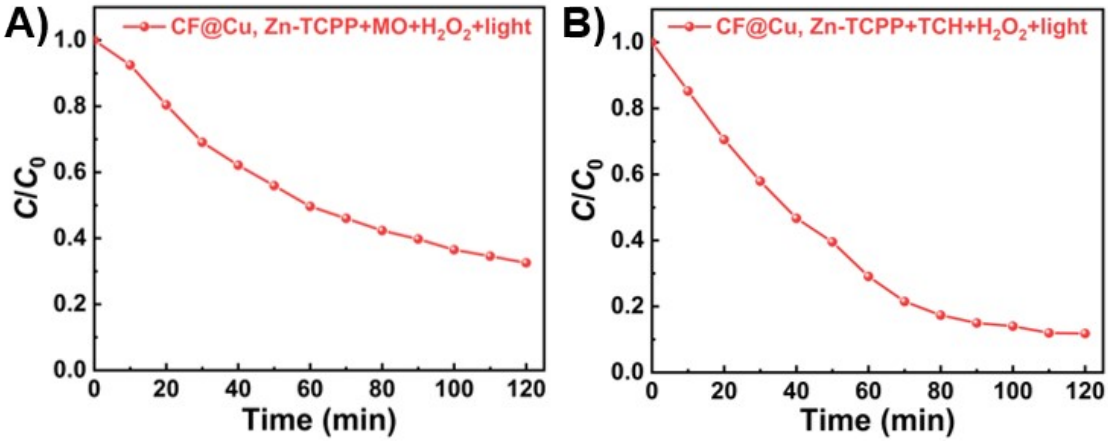

Figure S16. The corresponding decomposition curves of **A)** MO and **B)** TCH by CF@Cu, Zn-TCPP via a photo-Fenton like degradation process.

References

1 Y. Wang, M. Zhao, J. Ping, B. Chen, X. Cao, Y. Huang, C. Tan, Q. Ma, S. Wu, Y. Yu, Q. Lu, J. Chen, W. Zhao, Y. Ying, H. Zhang, *Adv. Mater.,* 2016, **28**, 4149-4155.

2 J. Chang, J. Ma, Q. Ma, D. Zhang, N. Qiao, M. Hu, H. Ma, *Appl. Clay Sci.,* 2016, **119**, 132-140.

3 D.-W. Cho, J. Lee, Y.S. Ok, E.E. Kwon, H. Song, *Chemosphere*, 2016, **163**, 305-312.

4 Q. Fu, D. Shi, C. Mo, J. Lou, S. Zhou, L. Zha, J. Wang, W. Yan, J. Luo, *J. Solid State Chem.*, 2022, **311**, 123100.

5 J. Li, L. Zhou, Y. Song, X. Yu, X. Li, Y. Liu, Z. Zhang, Y. Yuan, S. Yan, J. Zhang, *Carbohydr. Polym.*, 2021, **270**, 118340.

6 Q. Wang, E.O. Fagbohun, H. Zhu, A. Hussain, F. Wang, Y. Cui, *Sep. Purif. Technol.*, 2023, **321**, 124205.

7 Y. Zhang, Y. Zheng, Y. Yang, J. Huang, A.R. Zimmerman, H. Chen, X. Hu, B. Gao, *Bioresour. Technol.*, 2021, **337**, 125432.

8 D.B. Jiang, C. Jing, Y. Yuan, L. Feng, X. Liu, F. Dong, B. Dong, Y.X. Zhang, *J. Colloid Interface Sci.*, 2019, **540**, 398-409.

9 L. Han, Y. Wu, K. Fang, S. Sweeney, U.K. Roesner, M. Parrish, K. Patel, T. Walter, J. Piermattei, A. Trimboli, J. Lefler, C.D. Timmers, X.-Z. Yu, V.X. Jin, M.T. Zimmermann, A.J. Mathison, R. Urrutia, M.C. Ostrowski, G. Leone, *Nat. Commun.*, 2023, **14**.

10 M.N. Nimbalkar, B.R. Bhat, *J. Environ. Chem. Eng.*, 2021, **9**, 106216.
11 E. Haque, J.W. Jun, S.H. Jhung, *J. Hazard. Mater.*, 2011, **185**, 507-511.
12 L. Ai, C. Zhang, Z. Chen, *J. Hazard. Mater.*, 2011, **192**, 1515-1524.
13 S. Li, T. Lei, F. Jiang, M. Liu, Y. Wang, S. Wang, X. Yang, *J.Colloid Interface Sci.*, 2020, **560**, 321-329.